Fifth International Symposium on Marine Propulsors
smp'17, Espoo, Finland, June 2017

Simulate the PPTC propeller with a vortex particle-boundary element hybrid method

Youjiang Wang[1], Moustafa Abdel-Maksoud[2], Peng Wang[1], Baowei Song[1]

[1]School of Marine Science and Technology, Northwestern Polytechnical University, Xi'an, P.R. China
[2]Institute for Fluid Dynamics and Ship Theory, Hamburg University of Technology, Hamburg, Germany

ABSTRACT

To investigate the possibility of using VPM in the marine propeller flow simulation, this work applies a hybrid method coupling the boundary element method and the vortex particle method to analyze the flow around the Potsdam Propeller Test Case (PPTC) propeller. The boundary element method is used to model the blade surface while the vortex particle method is used for the wake flow field. The results show that the open water characteristics obtained with the developed hybrid method correlate very well with the experimental result. The obtained tip vortex position and velocity distribution also correlates well with the experimental measurement qualitatively. The computational time is also presented and compared with other methods.

Keywords

marine propeller, vortex particle method, BEM-VPM hybrid method.

1 INTRODUCTION

For the analysis of noise, interaction and off-design working conditions of the marine propeller, it is always essential to get the accurate prediction of the flow details, especially the vortex structures in the flow. Existing technique includes using RANS or DES solver to solve the flow detail, which is quite successful in recent years. Besides, to predict the leading edge vortex and tip vortex efficiently, Tian & Kinnas (2015) presented a VIScous Viscosity Equation solver, in which the concentration of vorticity is exploited and the viscous vorticity equation is solved with finite volume method in a small region around the propeller blade. Far downstream vortex wake is modeled with potential wakes and velocity boundary condition is utilized to consider the mutual influence. The current work is aimed to investigate the possibility of applying vortex particle method (VPM) in the simulation of the flow around marine propellers.

The VPM is a scheme designed especially for the vortex analysis. It is based on the Lagrangian discretization of the vorticity transport equation. The vorticity field is discretized with a set of Lagrangian vortex particles. The particles carry the vorticity, move with the field velocity and only exist in the region where the vorticity is not negligible. The Lagrangian discretization makes VPM free from the numerical diffusion, which is always suffered by the grid-based solvers.

Because of the advantages of VPM in the vortex simulation, it has been adopted for various simulations relating to vortices. Mammetti et al (1999) adopted VPM to study the collision of a vortex ring with a solid wall for the investigation of the artificial noise. The obtained numerical vortex structure agreed very well with the experimental visualization. The instability of two pairs of counter rotating vortices in the aircraft wake has been simulated using VPM by Chatelain et al (2008). The Ω-shape loops formed by the main and secondary vortices, which is typical in the medium wavelength instability, have been reproduced in simulation, and the evolution of longitudinal energy modes (along the stream-wise direction) correlated well with those observed in experiments. VPM has also been used to model the wake field of wind turbine by Chatelain et al (2011), Backaert et al (2015), and Branlard et al (2016). In their works, the wind turbine blades are modeled with lifting lines and the shedding vorticity is modeled with vortex particles. However, VPM has not yet been used to analyze the flow around marine propellers.

VPM is to be applied for the simulation of marine propeller flow in this work. Because of the complexity of handling the boundary condition in VPM, in the current work it is coupled with the boundary element method (BEM). In the hybrid method BEM is used to model the blade surface and VPM is used to model the wake flow. BEM and VPM are described briefly in the following section. The coupling scheme is introduced in section 3. In section 4, the hybrid method is used to analyze the PPTC propeller and the results are given. In section 5, the main conclusions of the current work are stated.

2 EXISTING METHODS

3.1 Boundary Element Method

In the current work, a low order in-house BEM code is adopted. In the BEM code, the field velocity consists of the free stream velocity and the disturbed velocity. The disturbed velocity is induced by the singularities on the body surface and the wake surface. The singularities on

the body panels are dipole and source, while on the wake panels there is only dipole, as shown in Figure 1. The strengths of the singularities are determined with the boundary conditions stating that the disturbed potential inside the body surface is zero.

On the body surface, the tangential component of the disturbed velocity is obtained by evaluating the disturbed potential's surface gradient. The pressure is computed according to the Bernoulli equation. The viscous force is evaluated using an empirical formula which relates the viscous shear stress to local Reynolds number and velocity, i.e.

$$\boldsymbol{F}_f = 0.5\rho S_p C_f |\boldsymbol{u}|\boldsymbol{u} \tag{1}$$

where $\boldsymbol{F}_f$ is the viscous force acting on a panel, S_p is the area of the panel, ρ is the water density, $\boldsymbol{u}$ is the total relative fluid velocity on the panel and C_f is the friction coefficient. According to Schlichting (1987), C_f can be evaluated as

$$C_f = (\log_{10} \mathrm{Re} - 0.65)^{-2.3} \tag{2}$$

where Re is the local Reynolds number on the panel.

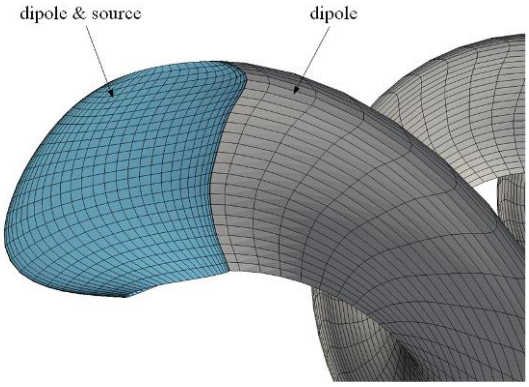

Figure 1 The distribution of singularities in the adopted in-house BEM code.

With the pressure and viscous force, the thrust and torque of the propeller can be obtained.

For the unsteady case, the wake panels are moved with the total field velocity. For the steady case, the wake is aligned with a faster algorithm, i.e., the DAM scheme stated in Wang et al (2016a).

For more details about the BEM code, please refer to Wang et al (2016a), Wang et al (2016b), and Wang et al (2017a).

3.2 Vortex Particle Method

The VPM is based on the vorticity transport equation (or the vorticity-velocity formation of the NS equation), which is

$$\frac{\mathrm{D}\boldsymbol{\omega}}{\mathrm{D}t} = (\nabla \boldsymbol{u})\cdot\boldsymbol{\omega} + \nu\Delta\boldsymbol{\omega} \tag{3}$$

where t is the time, $\boldsymbol{u}$ is the velocity, v is the kinematic viscosity and $\boldsymbol{\omega} = \nabla \times \boldsymbol{u}$ is the vorticity. The vorticity field is discretized with a set of Lagrangian vector – valued particles, i.e.

$$\boldsymbol{\omega}(x) = \sum_p \boldsymbol{\alpha}_p \zeta_\varepsilon(\boldsymbol{x} - \boldsymbol{x}_p) \tag{4}$$

where $\boldsymbol{x_p}$ and $\boldsymbol{a}_p$ represent the positions and strengths of particles, respectively, and ζ_ε stands for the mollification function which depends on the particle's core size ε. The mollification function is defined as

$$\zeta_\varepsilon(\boldsymbol{x}) = \frac{1}{\varepsilon^3}\zeta(\frac{|\boldsymbol{x}|}{\varepsilon}) . \tag{5}$$

In this work, the Gaussian mollification function is adopted for ζ , i.e.

$$\zeta(\lambda) = \frac{1}{(2\pi)^{3/2}}\exp(-\frac{\lambda^2}{2}) . \tag{6}$$

The particle strength is the total vorticity contained in the particle's volume, i.e.

$$\boldsymbol{\alpha}_p = \int_{V_p} \boldsymbol{\omega} \mathrm{d}V \tag{7}$$

where V_p denotes the volume associated with the particle p.

Discretize the vorticity transport equation with vortex particles, the formulas governing the VPM simulation are obtained as

$$\frac{\mathrm{d}\boldsymbol{x}_p}{\mathrm{d}t} = u(\boldsymbol{x}_p) \tag{8}$$

$$\frac{\mathrm{d}\boldsymbol{\alpha}_p}{\mathrm{d}t} = \nabla \boldsymbol{u}(\boldsymbol{x}_p)\cdot\boldsymbol{\alpha}_p + V_p \nu \Delta\boldsymbol{\omega}(\boldsymbol{x}_p) \tag{9}$$

In Equation (9), $\nabla \boldsymbol{u}\cdot\boldsymbol{\alpha}$ is called the vorticity stretching term while $V\nu\Delta\boldsymbol{\omega}$ is called the viscous diffusion term. The local velocity $\boldsymbol{u}$ consists of the free stream velocity and the disturbed velocity. The disturbed velocity is the summation of the induced velocity from every vortex particle as follows

$$\boldsymbol{u}_i(\boldsymbol{x}) = \sum_p \boldsymbol{K}_\varepsilon(\boldsymbol{x} - \boldsymbol{x}_p)\times\boldsymbol{\alpha}_p \tag{10}$$

where $\boldsymbol{K}_\varepsilon$ is the velocity kernel, which is obtained by applying the Biot-Savart theory to the mollified vortex particle. The gradient of the velocity is

$$\nabla\boldsymbol{u}_i(\boldsymbol{x}) = \sum_p \nabla\boldsymbol{K}_\varepsilon(\boldsymbol{x} - \boldsymbol{x}_p)\times\boldsymbol{\alpha}_p . \tag{11}$$

The viscous diffusion term (especially the Laplacian operator Δ) cannot be evaluated directly in the particle system. In the current work, the particle strength exchange technique developed by Degond & Mas-Gallic (1989) is adopted for the relative calculation.

As the simulation advances, the flow's local strain always leads to particles clustering in one direction and spreading in other directions. The non-uniform distribution may

endanger the convergence and stability of VPM. Thus, it is necessary to redistribute the vortex particles to regular positions. In the current work, the 3D interpolation using the Cartesian product of M_4' function is adopted to obtain the strengths of the new particles.

In the engineering related applications, the inter-particle spacing may not be small enough to capture all the turbulence scales. In such cases, sub-grid scale dissipation model is needed to consider the influence of the under-resolved scale dissipation. In the current work, the artificial viscosity model promoted by Cottet (1996) especially for VPM is adopted.

For more details about the VPM, please refer to Wang et al (2017b), Cottet & Koumoutsakos (2000), and Ploumhans et al (2002).

3 THE HYBRID METHOD

3.2 Coupling Scheme

The current work couples the BEM and VPM together to calculate the marine propeller flow, as shown in Figure 2. The BEM is used to model the propeller surface and the VPM is used to model the wake flow. Two columns of wake panels are left as the buffer wake.

The buffer wake is used to connect the BEM and VPM systems. In the BEM system, the buffer wake is used to satisfy the Kutta condition and close the equation system. In each time step, a new column of wake panels are shed from the trailing edge and the last column are converted to vortex particles. The conversion is based on the relationship between dipole distribution and vorticity,

$$\boldsymbol{\omega} = \boldsymbol{n} \times \nabla_s \mu \tag{12}$$

where μ is the dipole strength on the panel, $\boldsymbol{n}$ is the unit normal vector and ∇_s denotes the surface gradient on the panel. In the low order panel method, the dipole strength is constant on one wake panel, which means the vorticity strength obtained with Equation (12) is zero. In the current work, the dipole strength on a panel is regarded as the value at the panel's center, and 2D interpolation is applied to construct a continuous non-constant distribution of the dipole strength on the wake surface.

To consider the influence of the VPM system on the BEM system, the vortex particles' induced velocities on the body panels are calculated. These velocities are regarded as a part of the free stream velocity when the source strengths are evaluated and as a part of the disturbed velocity when the pressure is evaluated. In the movement of the buffer wake panels, the vortex particles' induced velocity is also included in the total field velocity.

To consider the influence of the BEM system on the VPM system, the panels' induced velocities at the particles' positions are evaluated and regarded as free stream velocity. At the same time, the gradients of the induced velocities are also evaluated for the computation of the vorticity stretching term.

3.2 Rotational Periodic Boundary

For the simulation of propellers, to reduce the computational time, only a subdomain corresponding to one blade is modeled. The rest are modeled with the rotational periodic boundary condition. As particles move out the subdomain from one periodic boundary, corresponding new ones are created and come in from the other periodic boundary. When the induced velocities are computed, the contribution of the rest domain is included by creating virtual particles according to the periodic condition.

The cross-section of the modeled subdomain is a sector. For the particle redistribution, regular hexahedral cells are generated in the modeled subdomain and new particles are placed at the cell centers. The inter-particle spacing h is utilized to control the particle density. Along the axial and radial directions, uniform grids with space being h are used. Every radial strip is divided to a specific number of uniform cells so that the cell's tangential length is around h, as shown Figure 3.

In the coupling method, to avoid particle piercing into the body, the particle redistribution is not carried out for the whole domain, but for the domain after a certain position. Such a treatment can also help reduce particle number and save computational time.

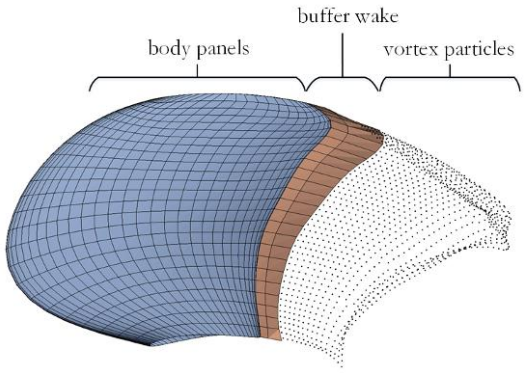

Figure 2 Different computational elements in the vortex particle-boundary element hybrid method.

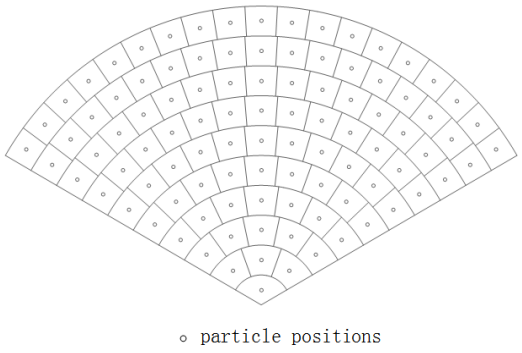

Figure 3 The uniform particle distribution on the sector-shape cross section.

4 NUMERICAL RESULTS

The open water characteristics of the PPTC propeller are evaluated using BEM and the hybrid method, respectively. The orthogonal panel arrangement is used on the propeller blade, as shown in Figure 4. The panel numbers along the chordwise and radial direction are 60 and 25, respectively. The time step is set so that the propeller rotates 6 degrees every step. The geometry of the PPTC propeller is given in Heinke (2011).

In the hybrid method, the particle's core size determines the range in which the particle distributes its vorticity. For the propeller wake, it is assumed that such a range approximately equal to the boundary layer thickness near the trailing edge. In this work, the particle core size ε is set around the boundary layer thickness at r/R=0.7, which is evaluated according to Schlichting (1987) as

$$\delta = 0.154\,\mathrm{Re}^{-1/7}\,C \qquad (13)$$

where Re is the local Reynolds number and C is the chord length. The inter-particle spacing h is set to be 1.2ε.

In the simulation, the particle redistribution beginning position is $0.4D$ after the propeller disk, where D denotes the propeller's diameter. To control the increase of particle number, the particle will be deleted when it goes further than $1.5D$ after the propeller disk. To achieve the convergent results, 300 steps are simulated from the beginning without any wake panels and vortex particles. The convergence history of the thrust and torque coefficient for the case with J=1.0 are shown in Figure 5. The particles distributions during the calculation and in the final step are given in Figure 6. It can be concluded that 300 steps are enough to obtain the final convergent result.

The obtained open water characteristics are given in Figure 7 together with the experimental result. The prediction of the hybrid method is more accurate than that of BEM, especially for low advance ratios. This is because the hybrid method models the wake flow more physically, which takes consideration of the shedding wake's thickness and the viscous diffusion. Figure 8 shows the comparison between the shapes of the vortex wakes obtained with BEM and hybrid method at J =1.0. Obvious differences are observed in the inner region. The vortex wake obtained with BEM is located further to the downstream. The different wake shapes then lead to different open water characteristics.

To investigate the influence of the particle redistribution beginning position and the particle deleting position on the predicted open water performance and the wake flow detail, three simulations with different configurations are carried out with the hybrid method for the PPTC propeller at J=1.0. The configurations are listed in Table 1, where the obtained open water characteristics are also given. The particle redistribution beginning position x_{rds} has little effect on the predicted open water performance. The difference is less than 0.1%. The particle deleting position x_{del} (or the computational domain's length) has a much larger influence. For the two cases with x_{del}=1.5D and

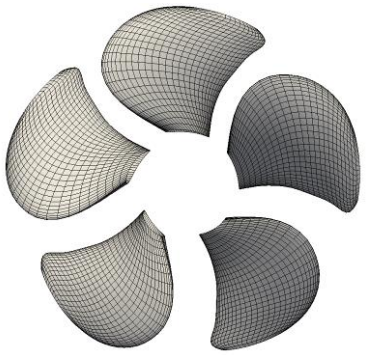

Figure 4 The panel arrangement on the propeller blade.

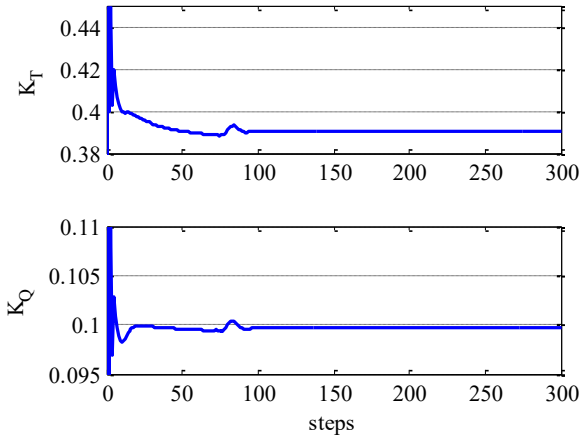

Figure 5 Convergence history of the thrust coefficient and torque coefficient in the hybrid method (for PPTC propeller at J=1.0).

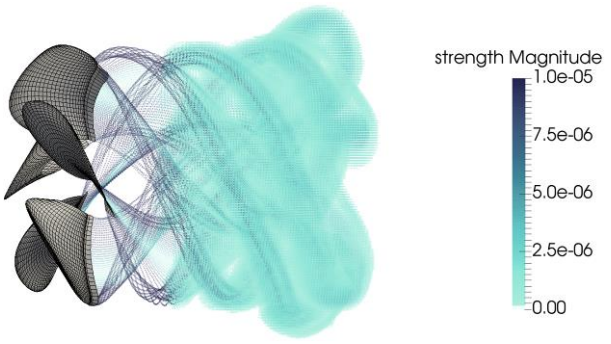

(a) 48th step

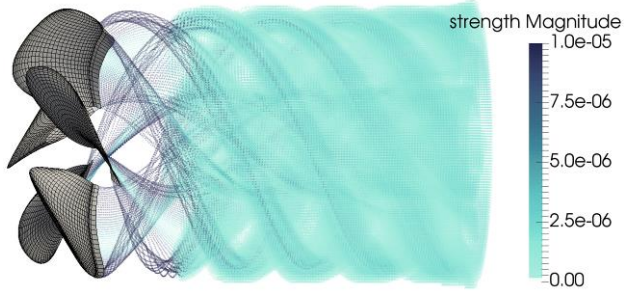

(b) 300th step

Figure 6 Particle distributions during the calculation. The color is defined by the particle's strength magnitude (for PPTC propeller at J=1.0).

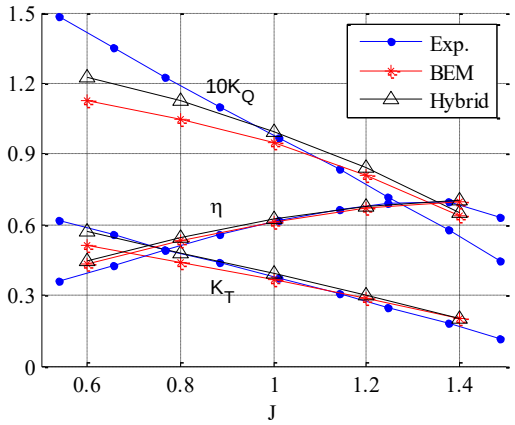

Figure 7 Open water characteristics of the PPTC propeller predicted by different methods.

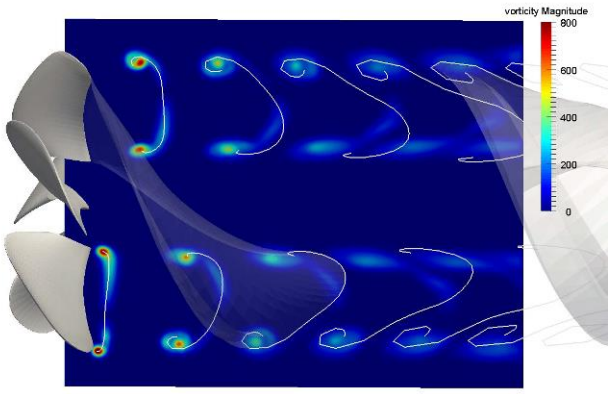

Figure 8 Shapes of the flow-adapted vortex wakes obtained with BEM (the white line) and hybrid method (the contours) at J =1.0.

x_{del}=1.0D, the differences between the predicted thrust and torque coefficient are around 1%.

The vortex structures obtained with the three afore-mentioned configurations are given in Figure 9 in the form of the vorticity strength iso-surfaces. Although with different particle redistribution beginning positions the open water characteristics are almost the same, the vorticity strengths are quite different. With a larger x_{rds}, all the iso-surfaces are conserved for a longer distance. The reason is that the interpolation scheme used in the particle redistribution process has numerical diffusion effects. A smaller x_{rds} means earlier particle redistribution, which results in an earlier influence of the numerical diffusion. The particle deleting position has little impact on the vorticity strength in the computational domain. The difference is only that the iso-surfaces are cut off by the rear boundary, i.e. the plane defined by x=x_{del}.

Furthermore, the helical trajectory of the tip vortex shown in Figure 9 qualitatively correlates well with the tip vortex trajectory observed in experiment, as shown in Figure 10. However, currently the quantitative comparison has not yet been carried out.

Table 1 Configurations and results of different cases for the simulation of the PPTC propeller at J =1.0.

	x_{rds}*	x_{del}**	K_T	$10K_Q$	η
case 1	0.4D	1.5D	0.3902	0.9967	62.3%
case 2	0.15D	1.5D	0.3900	0.9965	62.3%
case 3	0.4D	1.0D	0.3941	1.0033	62.5%

* x_{rds} denotes the particle redistribution beginning position;

** x_{del} denotes the particle deleting position.

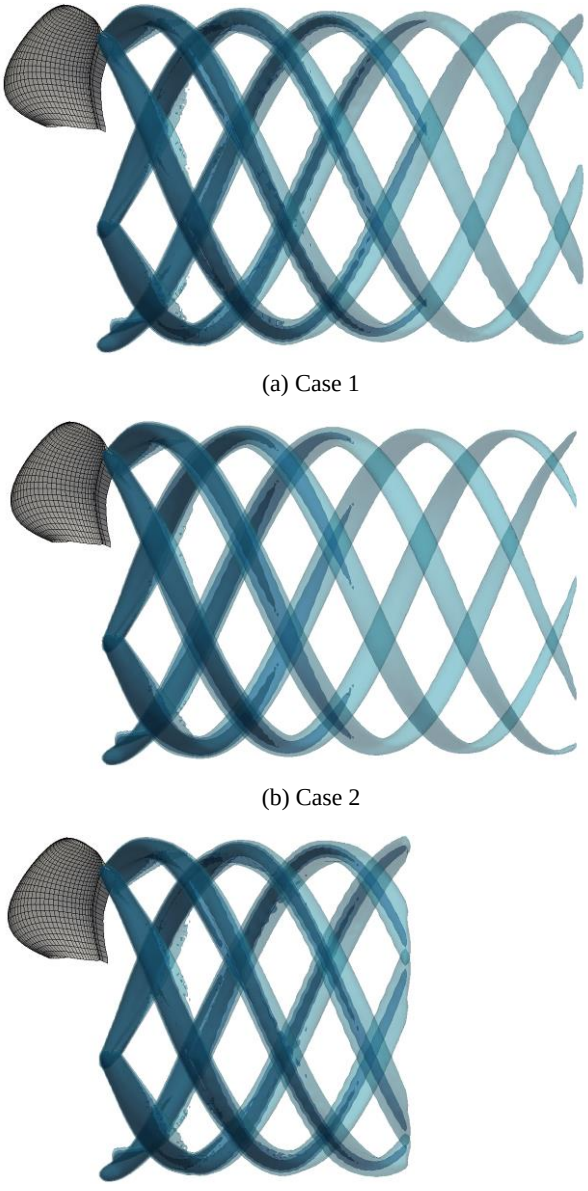

(a) Case 1

(b) Case 2

(c) Case 3

Figure 9 The iso-surfaces of the vorticity strength for different configurations listed in Table 1. The advance ratio is J=1.0, and the values for the iso-surfaces are $|\boldsymbol{\omega}|$= 150s^{-1}, 200s^{-1}, 250s^{-1}.

In Table 2, configurations of simulations with different inter-particle spacing and the obtained results are listed. A smaller inter-particle spacing means a higher particle density, and will lead to a larger number of particles and longer computational time. With the results listed in Table

Figure 10 Experimental observation of the tip vortex cavitation, which reflects the trajectory of the tip vortex (taken from Heinke (2011)).

2, it can be found that increasing the inter-particle spacing will cause an decrease in K_T and K_Q, however, the differences are quite small (less than 0.3%). Thus, the inter-particle spacing (or particle number) has little influence, if any, on the predicted K_T and K_Q.

However, the inter-particle spacing has a noticeable influence on the vorticity strength, as shown in Figure 11. A smaller inter-particle spacing leads to a stronger vorticity in the wake flow field. Actually, the voriticy strength is directly affected by the particle core size ε, which determines the range of the vorticity distribution. Such a range should be correlated to the boundary layer thickness, as given by Equation (13).

Table 2 Results of the simulations with different inter-particle spacing h for PPTC propeller at J =1.0.

	ε	h	K_T	$10K_Q$	η	T_{step}*
case 1	0.01D	0.011D	0.3902	0.9967	62.3%	181s
case 2	0.015D	0.016D	0.3895	0.9948	62.3%	30s
case 3	0.02D	0.021D	0.3890	0.9937	62.3%	15s

* T_{step} denotes the averaged computational time for every step.

The flow around PPTC propeller has also been simulated with the commercial RANS solver CFX. In the simulation, the rotational periodic boundary condition is used and only one blade is simulated. The whole computational domain consists of a rotational domain surrounding the blade and a static outer domain. For the rotational domain 802K hexahedral cells are used and for the static domain 523K cells are used. The k-ω SST model is adopted for the turbulence model. 500 steps are simulated to achieve the final convergent result.

Vortex structures obtained with CFX and the hybrid method are given in Figure 12. The hybrid method leads to thinner iso-surfaces, which means at the beginning position the vorticity strength is smaller than that obtained with CFX. This may results from the too large particle core size used in the panel-to-particle conversion process.

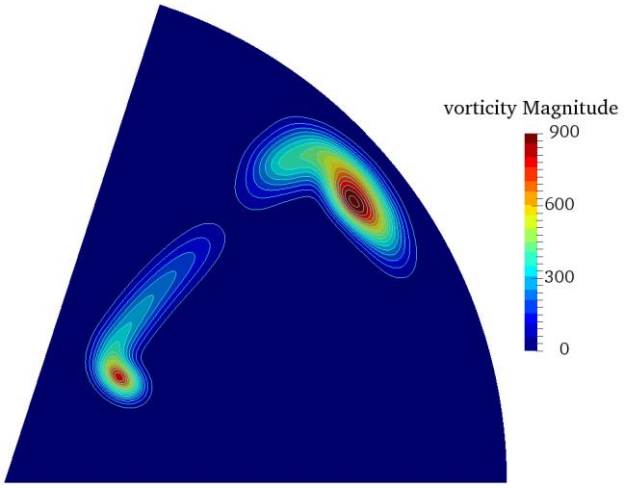

(a) Case 1, h=0.011D

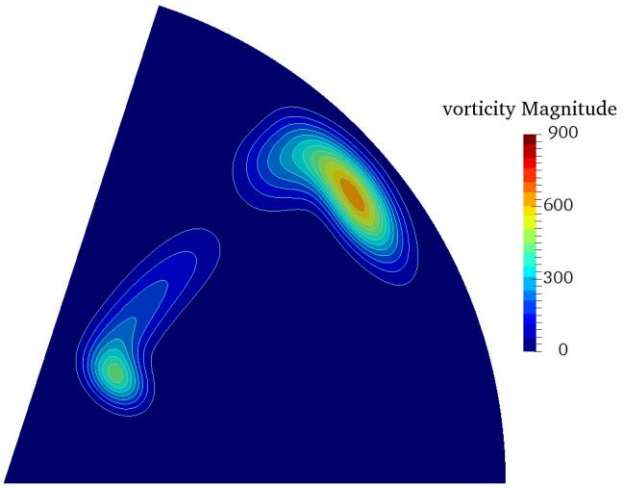

(b) Case 2, h=0.016D

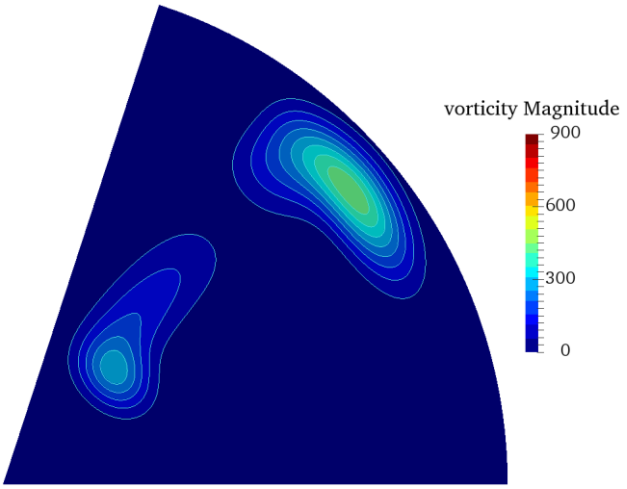

(c) Case 3, h=0.021D

Figure 11 The vorticity strength on the plane located 0.16D after the propeller disk obtained by different simulations listed in Table 2 (the advance ratio is J =1.0).

Further investigation of the conversion process will probably improve the correlation. In addition, the radius of iso-surfaces obtained with the hybrid method decreases

much slower, which means the hybrid method has a better ability to conserve the vorticity than the RANS solver, at least with current configurations. Besides, the iso-surfaces obtained with CFX are discontinuous near the interface while those obtained with the hybrid method are continuous and smooth.

The distribution of the axial velocity on the plane located 0.2D after the propeller disk is given in Figure 13 together with the experimental measurement by Mach (2011). The tip vortex positions correlate very well. The small inward offset is because that in BEM 1% of the blade is cut out at the tip. The velocity gradient obtained with the hybrid method is smaller than that observed in the experiment. This indicates that with the current configuration, the calculated concentration of the vorticity is not enough. To obtain a more accurate prediction of the velocity field, a higher particle density is needed.

The computational time of different methods is listed in Table 3. The current hybrid method is not a time-saving method. However, the particle density does not influence the predicted open water characteristics very much. A larger inter-particle spacing could reduce the total simulation time within 2 hours. On the other side, a more accurate prediction of the flow detail needs a smaller inter-particle spacing and more computational time. Furthermore, the algorithm to improve the computational efficiency is also under research.

Table 3 The computational time for different methods.

	Total Time	Steps	Averaged time per step
Hybrid Method	15.1h	300	181s
BEM	74.0s	9	8.24s
CFX	4.72h	500	34s

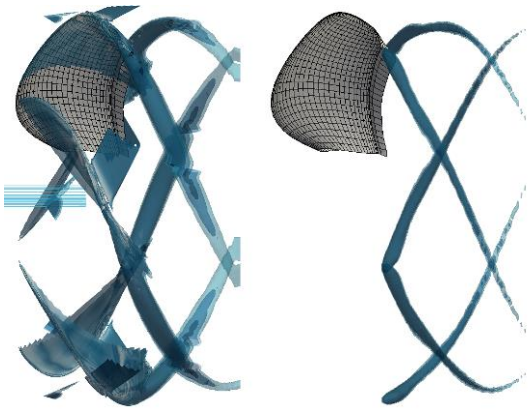

(a) CFX (b) Hybrid method

Figure 12 Comparison between CFX result and Coupling method. The advance ratio is J=1.0, and the values for the iso-surfaces are $|\omega|$= 500s^{-1}, 550s^{-1}, 600s^{-1}.

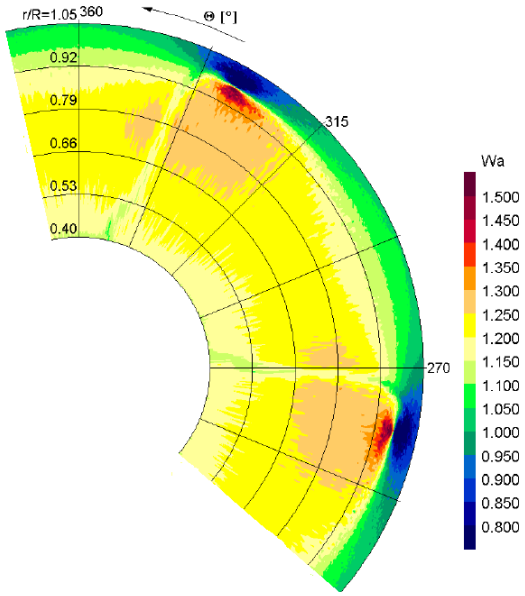

(a) Experimental measurement (taken from Mach (2011)).

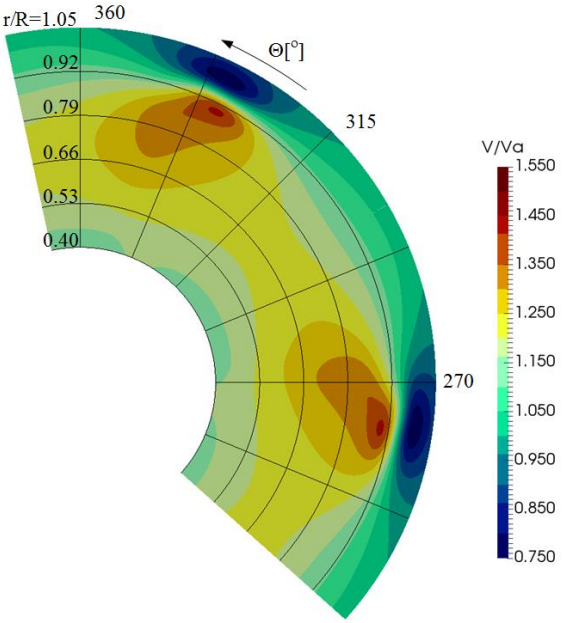

(b) Obtained with the hybrid method.

Figure 13 The distribution of non-dimensional axial velocity on the plane located 0.2D after the propeller disk. The velocity is nondimensionalized by the propeller's advance velocity V_a.

4 CONCLUSIONS

In this work, a hybrid method combining the boundary element method and the vortex particle method is used to simulate the flow around the PPTC propeller. The blade surface and non-penetrating boundary condition is modeled by boundary element method, while the vortex wake is modeled by viscous vortex particle method.

The results obtained with the hybrid method are encouraging. The obtained thrust and torque coefficient are more accurate than our in-house BEM code. Although the relative merit between hybrid method and BEM may

be different for other BEM codes, the hybrid method gives a quite competitive result in current stage. The obtained vorticity and velocity field correlates well qualitatively with the flow field obtained by experiment and RANS solver.

In the future, further investigation of the panel-particle conversion process will be carried out. The algorithm to reduce the computational time is also needed to be investigated. Then, more quantitative comparison with experiment and other methods will be presented.

REFERENCES

Backaert, S., Chatelain, P. & Winckelmans, G. (2015). 'Vortex particle-mesh with immersed lifting lines for aerospace and wind engineering'. IUTAM Symposium on particle methods in fluid mechanics, Gotland, Sweden.

Branlard, E., Mercier, P., Machefaux, E., Gaunaa, M. & Voutsinas, S. (2016). 'Impact of a wind turbine on turbulence: Un-freezing turbulence by means of a simple vortex particle approach'. Journal of Wind Engineering and Industrial Aerodynamics 151, pp.37-47.

Chatelain, P., Bricteux, L., Backaert, S., Winckelmans, G., Kern, S. & Koumoutsakos, P. (2011). 'Vortex particle-mesh methods with immersed lifting lines applied to the Large Eddy Simulation of wind turbine wakes'. IUTAM Symposium on particle methods in fluid mechanics, Gotland, Sweden.

Chatelain, P., Curioni, A. Bergdorf, M., Rossinelli, D., Andreoni, W. & Koumoutsakos, P. (2008). 'Billion vortex particle direct numerical simulations of aircraft wakes'. Computer Methods in Applied Mechanics and Engineering 197, pp.1296-1304.

Cottet, G-H. (1996). 'Artificial viscosity models for vortex and particle methods'. Journal of Computational Physics 127(2), pp.299-308.

Cottet, G.-H. & Koumoutsakos, P. (2000). Vortex methods: theory and practice. Cambridge university press.

Degond, P. & Mas-Gallic, S. (1989). 'The weighted particle method for convection-diffusion equations. I. The case of an isotropic viscosity'. Mathematics of computation 53(188), pp.485-507.

Heinke, H.-J. (2011). 'Potsdam Propeller Test Case (PPTC): Cavitation tests with the model propeller VP1304'. Report 3753, Potsdam, Germany.

Mach, K.-P. (2011). 'Potsdam Propeller Test Case (PPTC): LDV velocity measurements with the model propeller VP1304'. Report 3754, Potsdam, Germany.

Mammetti, M., Verzicco, R. & Orlandi, P. (1999). 'The study of vortex ring/wall interaction for artificial nose improvement'. ESAIM: Proceedings 7, pp.258-269.

Ploumhans, P., Winckelmans, G., Salmon, J.K., Leonard, A., & Warren, M. (2002). 'Vortex methods for direct numerical simulation of three-dimensional bluff body flows: application to the sphere at Re=300, 500, and 1000'. Journal of Computational Physics 178(2), pp.427-463.

Schlichting, H. (1987). Boundary-layer theory. Mcgraw-Hill Book Company.

Wang, Y.J., Abdel-Maksoud, M. & Song, B. (2016a). 'Convergence of different wake alignment methods in a panel code for steady-state flows'. Journal of marine science and technology 21(4), pp.567-578.

Wang, Y.J., Abdel-Maksoud, M., Wang, K. & Song, B. (2016b). 'Prediction of tip vortex cavitation inception with low-order panel method'. Ocean Engineering 125, pp.124-133.

Wang, Y.J., Abdel-Maksoud, M. & Song, B. (2017a). 'A fast method to realize the pressure Kutta condition in boundary element method for lifting bodies'. Ocean Engineering 130, pp.398-406.

Wang, Y.J., Abdel-Maksoud, M. & Song, B. (2017b). 'Simulating marine propellers with vortex particle method'. Physics of Fluids 29(1), pp.017103.

Tian, Y. & Kinnas S. A. 'A viscous vorticity method for propeller tip flows and leading edge vortex'. Fourth international symposium on marine propulsors (smp'15), Austin, Texas, USA, June 2015.

DISCUSSION

Question from Stefano Brizzolara

How do you consider shear forces on the blades?

Author's closure

The shear forces on the blades are evaluated with an empirical formula. The local velocities on the blades surface are firstly achieved by the hybrid method described in the manuscript. Then the local Reynolds number is evaluated for every surface panel based on the local velocity and its surface distance to the leading edge. After that the equation (2) in the manuscript is used to calculate the shear force coefficient. With the coefficient, the shear force for each panel is evaluated using equation (1). Finally the shear forces are integrated around the blade to obtain the total shear force.